Available online at www.sciencedirect.com
SCIENCE DIRECT®
Journal of Power Sources 136 (2004) 37–44
JOURNAL OF POWER SOURCES
www.elsevier.com/locate/jpowsour

On the improved properties of injection-molded, carbon nanotube-filled PET/PVDF blends

Man Wu, Leon L. Shaw*

Department of Materials Science and Engineering, University of Connecticut, Storrs, 97 N. Eagleville Road, U-136, CT 06269, Connecticut, USA

Received 5 April 2004; accepted 30 April 2004

Available online 29 July 2004

Abstract

The mechanisms for improved mechanical and electrical properties of an injection molded, carbon nanotubes (CNTs) filled, polyethylene terephthalate (PET)/polyvinylidene fluoride (PVDF) blend have been investigated. It is found that the improved properties are due to the formation of a triple-continuous structure in the CNT-filled polymer blend; CNT segregates in the continuous PET phase, forming a continuous conductive path to provide the composite an electrical short circuit. The continuous PVDF phase free from CNT, on the other hand, offers crack bridging and the interface between the PET and PVDF phases provides crack deflection for the composite. As a result of such a combination, the CNT-filled PET/PVDF has better electrical conductivity, strength and elongation than the CNT-filled PET with the same CNT loading. The segregation of CNT in the PET phase of the CNT-filled PET/PVDF blend is due to the thermodynamic driving force that favors the segregation of CNT in the PET.

Keywords: PEM fuel cells; Bipolar plates; Carbon-filled polymers; Polymer blends

1. Introduction

Currently, bipolar plates of polymer electrolyte membrane (PEM) fuel cells are either made of Poco^{TM} graphite or carbon-filled polymers. However, the material and manufacturing costs of these bipolar plates are very high and need to be reduced by ~10 times before PEM fuel cells can be fully embraced for the automotive application [1]. For example, the cost of a graphite bipolar plate is currently about US$ 10 per plate if both the material and machining costs are included [2]. Such a high cost is due to the brittleness of graphite, which drives the machining cost of the flow channels on bipolar plates to a prohibitive level.

Extensive research has been conducted to search for low cost, high performance bipolar plates. These research efforts include studies of metal-based bipolar plates [3–6], carbon-filled polymers [7–9], and carbon/carbon composites [2]. However, these efforts have met limited success; either the performance is not satisfactory or the cost is still high [2–9]. For example, metal-based bipolar plates typically suffer from corrosion in the fuel cell environment, which results in a release of cations. The cations, in turn, lead to an increase in membrane resistance and to poisoning of the electrode catalysts [6]. In the case of carbon-filled polymers, high carbon loadings (typically > 50 vol.%) are needed in order to provide the required electrical conductivity [10,11]. As a result of such high carbon concentrations, utilization of injection molding, which is suitable for mass manufacturing and will result in low-cost bipolar plates [1], is precluded because of the difficulty in processability; instead, compression molding, which is a slow process because one must allow the mold to cool down before the part can be taken out, often becomes the only choice of processing method [10]. An additional problem associated with high carbon concentrations in polymers is the substantial reduction in the strength and ductility of the polymer composites. It is well known that the tensile strengths of polymer composites increase initially with the addition of a small amount of fillers (~5–20 vol.% CB), but decrease with higher filler loading [12–14]. Such phenomena have normally been attributed to the weak filler-matrix interface [12].

Recently, we have proposed a concept of making carbon-filled polymer blends containing a triple-continuous structure in 3D space [15,16]. Fig. 1 shows the schematic of

* Corresponding author. Tel.: +1 860 486 2592; fax: +1 860 486 4745.
E-mail address: 1shaw@mail.ims.uconn.edu (L.L. Shaw).

0378-7753/$ – see front matter © 2004 Elsevier B.V. All rights reserved.
doi:10.1016/j.jpowsour.2004.04.016

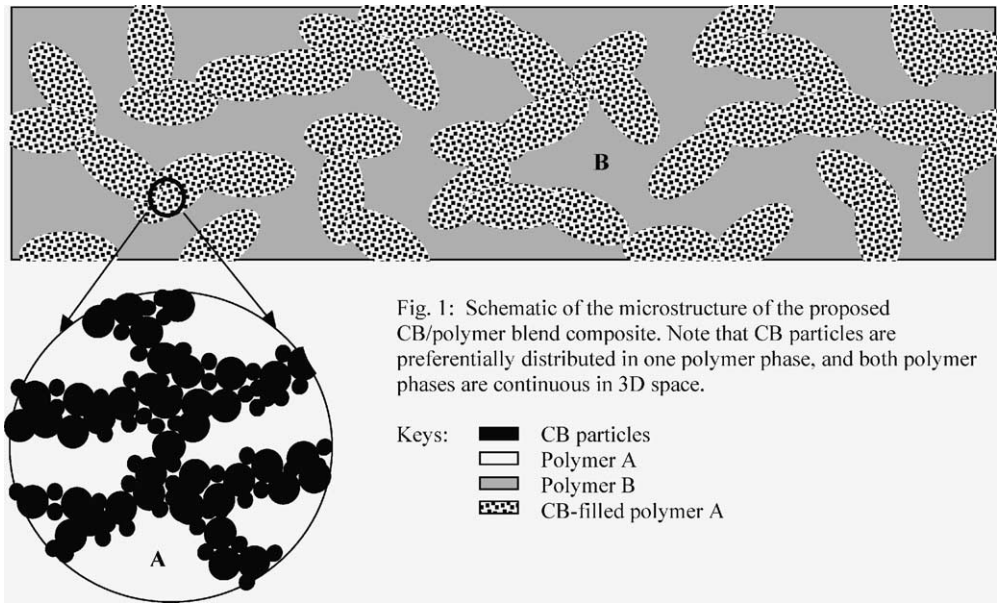

Fig. 1. Schematic of the microstructure of the proposed CB/polymer blend composite. Note that CB particles are preferentially distributed in one polymer phase, and both polymer phases are continuous in 3D space.

such a carbon-filled polymer blend, which consists of a binary polymer blend both phases of which (i.e., Phases A and B in Fig. 1) are continuous in 3D space. The conductive carbon is preferentially located in one phase (Phase A in Fig. 1) and its concentration is high enough to form a continuous structure (i.e. at least higher than the percolation threshold in Phase A) so that a continuous electrical conductive path is present in the polymer. Such a triple-continuous structure has the advantage of achieving conductive polymer composites at lower carbon concentrations since only the percolation threshold in one phase, rather than the entire polymer blend, needs to be exceeded [17,18]. Such triple-continuous, carbon-filled polymer blends also offer two additional advantages, which are (i) the improved processability because of the low carbon concentration required, and (ii) minimal degradation in tensile properties because of the presence of a continuous neat polymer phase (Phase B in Fig. 1).

The feasibility of making triple continuous, carbon-filled polymer blends via injection molding has been demonstrated previously using a carbon nanotube (CNT) filled polyethylene terephthalate (PET)/polyvinylidene fluoride (PVDF) blend. The CNT-filled PET/PVDF blend exhibits 2500% improvement in electrical conductivity, 36% increase in tensile strength, and 320% improvement in elongation over the CNT-filled PET at the same carbon loading [16]. Thus, the triple continuous, carbon-filled polymer blends have great potentials for manufacture of low cost conductive polymers with superior conductivity and strength for bipolar plate applications of PEM fuel cells. To develop fundamental understanding of the improved properties of the CNT-filled PET/PVDF over the CNT-filled PET, additional experiments have been performed in this study. The results and analysis based on these new experiments are presented below.

2. Experimental

The detail of making the CNT-filled PET/PVDF blend and CNT-filled PET via injection molding can be found elsewhere [16] and will not be repeated here. Briefly, CNT was first extruded with PET to prepare masterbatches of PET pellets containing 12 vol.% CNT. These CNT-filled PET pellets were subsequently mixed with PVDF pellets in an 1–1 volume ratio and injection molded to form PET/PVDF blends containing 6 vol.% CNT. The PET containing 6 vol.% CNT was prepared in a similar manner, i.e. the extruded PET with 12 vol.% CNT was mixed with neat PET pellets in an 1-to-1 volume ratio and injection molded.

The electrical conductivity of CNT-filled polymers was measured using the two-probe dc method with a Solartron SI 1287 Electrochemical Interface. By applying 0.1 and 0.01 A currents, the corresponding voltages were measured. Based on the current, I, and the voltage, V, recorded, the electrical conductivity, σ, was calculated with the aid of

$$\sigma = \frac{\mathrm{d}I}{AV} \tag{1}$$

where d is the specimen thickness between the two electrodes and A is the cross-sectional area perpendicular to the current direction in the sample. Silver paste was utilized in all the measurements to ensure good contact of the sample surface with the electrodes of the electrochemical interface. Furthermore, the electrical conductivity was measured in two directions for the injection-molded rectangular plates (Fig. 2a); one was parallel to the injection flow direction (called Direction I hereafter) and the other perpendicular to the flow direction (called Direction II).

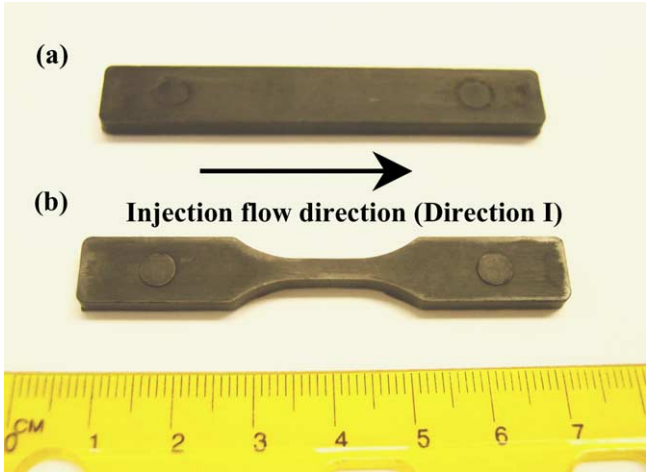

Fig. 2. Samples for (a) conductivity measurements and (b) tensile tests. The direction parallel to the injection flow direction is termed Direction I, whereas the direction perpendicular to the injection flow direction is called Direction II in the text.

Tensile specimens of PET, PVDF, and CNT-filled polymers with a gauge length of 10 mm (Fig. 2b) were injection molded and utilized to characterize the tensile properties. The tensile test was performed at a constant crosshead speed of 6 mm/min using a servo-hydraulic loading frame. An extensometer was attached to the gauge length of the sample to provide the strain value as a function of loading.

The morphology of polymer phases and the distribution of carbon nanotubes in the polymer blend were observed using an environmental scanning electron microscope (Phillips ESEM 2020). Specimens for the ESEM observation were prepared via polishing using Al_2O_3 suspension down to 0.05 μm, followed by ion etching using an Argon Ion Sputter Gun from Physical Electronic Industry, Inc., with a 3 kV voltage and a 45° angle of the sputter gun with respect to the specimen surface for 45 min. After ion-etching, gold coating was deposited to all the samples in order to avoid charging during SEM observation.

To provide hard evidence for deformation and fracture mechanisms, several CNT-filled PET/PVDF samples were loaded in tension and unloaded right before fracture. These samples were cut using a diamond saw in order to prepare a polished cross section that was parallel to the tensile loading axis. The polished cross section was subsequently ion etched using the conditions described previously to expose the presence of microcracks and their relative positions with respect to the PET and PVDF phases in the CNT-filled PET/PVDF blend.

3. Results and discussion

Fig. 3 shows the SEM images of the CNT-filled PET/PVDF blend after polishing and ion etching. Two distinct regions are noted; one contains carbon nanotubes (Region B) and the other is free of carbon nanotubes (Region A). The ratio of Regions A to B is about 1, consistent with the volume ratio of PET to PVDF. Recall that the CNT-filled PET/PVDF blends were prepared by pre-extrusion of carbon nanotubes with PET, followed by mixing and injection molding with neat PVDF. Thus, it is reasonable to conclude that Region A is the PVDF phase, whereas Region B is the PET phase containing CNT because transferring CNT into PVDF to create an 100% clean PET region during injection molding is very unlikely kinetically. The thermodynamic

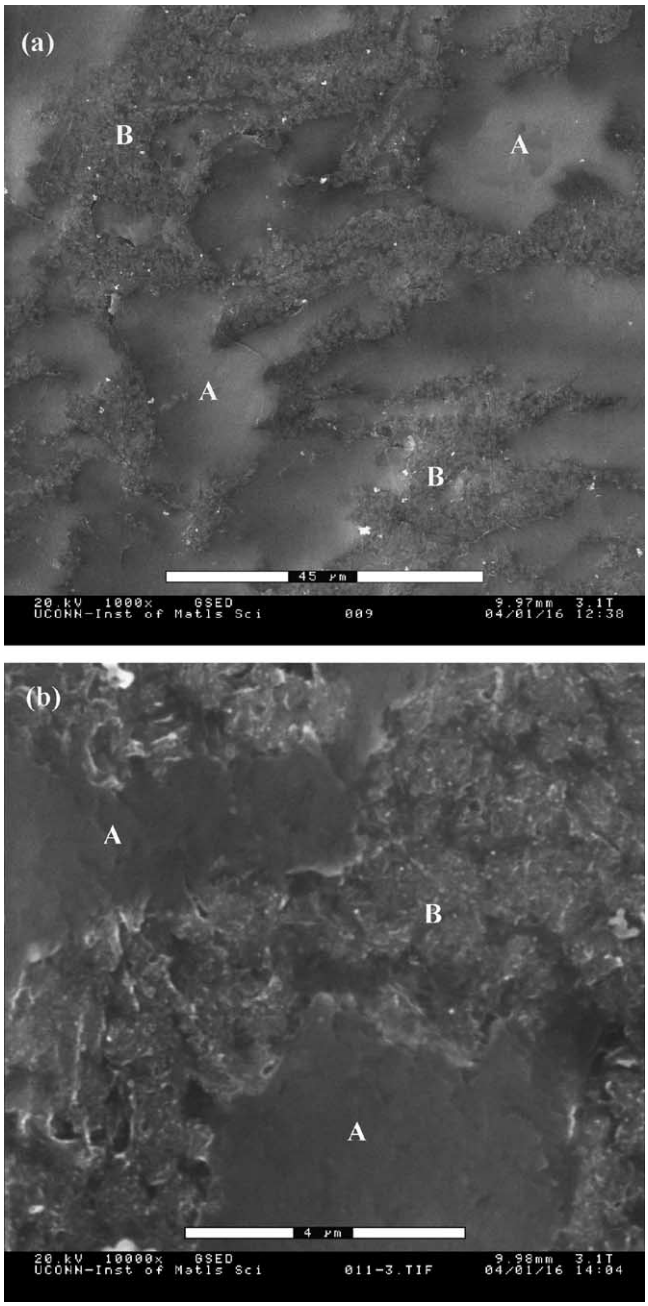

Fig. 3. SEM secondary electron image of (a) the ion-etched surface of the CNT-filled PET/PVDF blend, and (b) a higher magnification view. Region A is the PVDF phase, whereas Region B is the PET with CNT. The white spots in Region B are CNT.

consideration also support that CNT will stay in the PET phase during injection molding, as elaborated below.

The distribution of carbon particles (or nanotubes) in a polymer blend will be dictated by the state of the minimum interfacial energy if the equilibrium state is reached. Such a minimum interfacial energy state can be determined by Young's equation [19]

$$\omega_a = \frac{\gamma_{C-B} - \gamma_{C-A}}{\gamma_{AB}} \quad (2)$$

where ω_a is the wetting coefficient, and γ_{C-A}, γ_{C-B}, and γ_{A-B} are the interfacial energy between carbon and polymer A, carbon and polymer B, and polymers A and B, respectively. When $\omega_a > 1$, carbon particles distribute within polymer A. When $-1 < \omega_a < 1$, carbon particles distribute at the interface of the polymer blend. Finally, when $\omega_a < -1$, carbon particles distribute within polymer B. The interfacial energy between two phases, γ_{12} (for phases 1 and 2), in Eq. (2) can be estimated using the harmonic-mean equation [20]:

$$\gamma_{12} = \gamma_1 + \gamma_2 - 4\left[\frac{\gamma_1^d \gamma_2^d}{\gamma_1^d + \gamma_2^d} + \frac{\gamma_1^p \gamma_2^p}{\gamma_1^p + \gamma_2^p}\right] \quad (3)$$

where γ stands for the surface tension and subscripts 1 and 2 refer to phases 1 and 2, respectively. Further, $\gamma = \gamma^d + \gamma^p$, γ^d is the dispersion component of surface tension, and γ^p is the polar component. The harmonic-mean equation has been shown experimentally to be suitable for estimating the interfacial energy between low-energy materials, such as polymers, organic liquids, water, etc. [20]. Thus, Eq. (3) is utilized here to evaluate the interfacial energy between carbon and polymers. Based on the surface tension data of carbon, PET and PVDF as well as their dispersion and polar components at 180 °C [20], the interfacial energies between carbon and polymers at 180 °C are found as follows. $\gamma_{C-PVDF} = 21.45\,\text{ergs/cm}^2$, $\gamma_{C-PET} = 12.34\,\text{ergs/cm}^2$, and $\gamma_{PET-PVDF} = 1.78\,\text{ergs/cm}^2$. Substituting these interfacial energies into Eq. (2) results in a wetting coefficient of 5.1 if PVDF is chosen as phase B and PET as phase A in Eq. (2). Therefore, the consideration of the minimum interfacial energy predicts that carbon nanotubes should stay in the PET phase. Thus, the preferential distribution of CNT within PET observed in this study is in good agreement with the thermodynamic consideration.

For comparison, Fig. 4 shows the distribution of carbon nanotubes in the injection molded CNT-filled PET. Recall that this injection molded CNT-filled PET was prepared via a two-step method, i.e. 12 vol.% CNT was extruded with PET first using a twin-screw extruder and subsequently this extruded CNT-filled PET was injection molded with neat PET again to produce a CNT-filled PET with a final CNT loading of 6 vol.%. It is quite clear that CNT is uniformly distributed in the PET phase even though the composite was prepared via a two-step method. Thus, it can be concluded that the non-uniform distribution of CNT in the CNT-filled

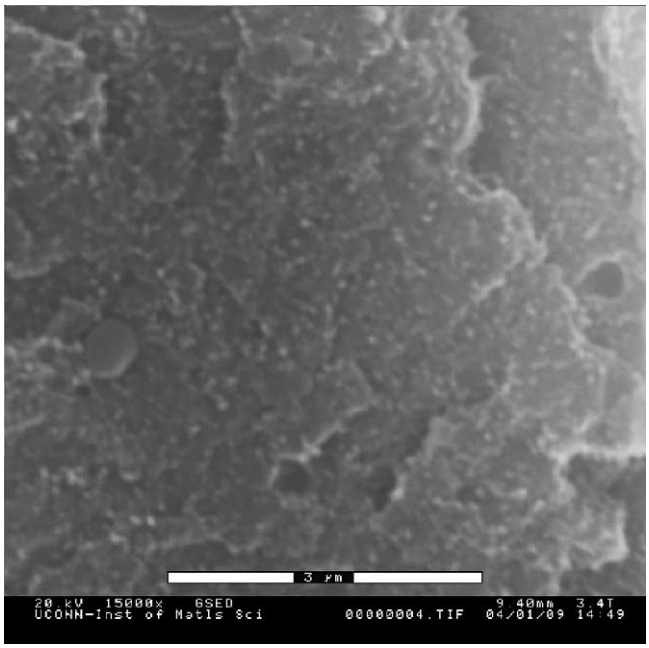

Fig. 4. SEM secondary electron image of a fracture surface of the CNT-filled PET fractured in liquid nitrogen, showing uniform distribution of CNT in the PET.

PET/PVDF blend is indeed due to the thermodynamic driving force that favors segregation of CNT in the PET phase.

Fig. 5 compares the stress–strain curves of neat PET, neat PVDF, PET with 6 vol.% CNT and PET/PVDF with 6 vol.% CNT. The major properties determined from these stress–strain curves for neat polymers and their CNT-filled composites are summarized in Table 1. Several features are noted from Fig. 5 and Table 1. First, the addition of CNT to the polymers has resulted in reductions in both tensile strength and elongation at break. For instance, the addition of 6 vol.% CNT to PET has led to a decrease in the tensile stress at break from 34 to 25 MPa and in the elongation at break from 2.2 to 1.2%. Second, as expected, the addition of CNT has increased the elastic modulus of PET. Furthermore, the modulus of the CNT-filled PET/PVDF blend falls between that of the CNT-filled PET and neat PVDF, as would be expected from the rule of mixtures for composites [21] since the CNT-filled PET/PVDF can be regarded as a composite made of CNT-filled PET and neat PVDF. Third, the CNT-filled PET/PVDF exhibits a 36% improvement in elongation and a 325% improvement in fracture strength over the CNT-filled PET with the same CNT loading. These improvements are due to the presence of the clean PVDF phase free from CNT in the CNT-filled PET/PVDF blend, as discussed below.

Shown in Fig. 6 are SEM images of crack paths in the CNT-filled PET/PVDF blend right before the fracture of the specimen. Note that cracks preferentially initiate and propagate within the CNT-filled PET phase. This is consistent with the stress–strain behaviors of the CNT-filled PET and neat PVDF shown in Fig. 5; that is, at strains slightly higher

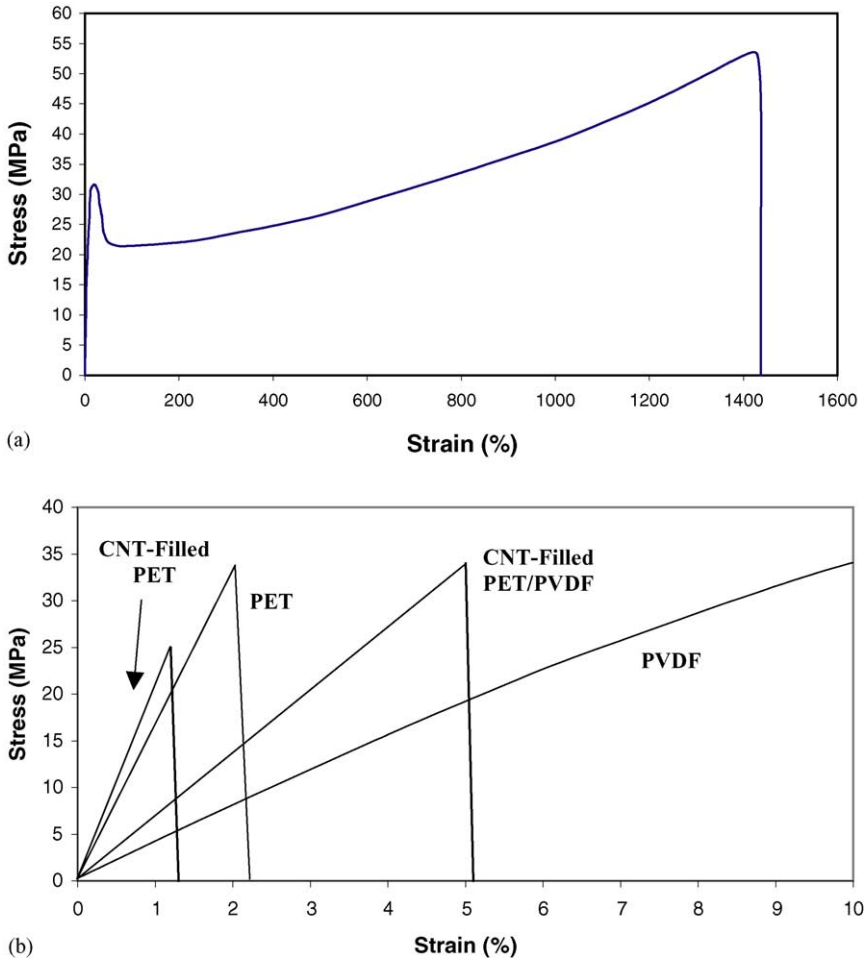

Fig. 5. Stress–strain curves of (a) PVDF and (b) PET, PET with 6 vol.% CNT, and PET/PVDF with 6 vol.% CNT. For comparison, part of the stress–strain curve of PVDF is also shown in (b).

than 1.2%, the CNT-filled PET phase will have cracks, while the clean PVDF phase can still carry the load because its elongation at break is ∼1400%. Thus, the presence of the clean PVDF phase free from CNT has provided strengthening mechanisms for the CNT-filled PET/PVDF blend. Such strengthening mechanisms are manifested as crack bridging and crack deflection at the PET/PVDF interface, as revealed in Fig. 6.

Assuming that the load after cracking of the CNT-filled PET phase is carried only by the clean PVDF phase, the fracture strength of the CNT-filled PET/PVDF would be ∼27 MPa because of the presence of 50 vol.% of the PVDF phase and its fracture strength of ∼54 MPa. The measured fracture strength of the CNT-filled PET/PVDF is 34 MPa (the average of three specimens), slightly higher than the prediction of the simple rule of mixtures. This discrepancy is likely due to the presence of the CNT-filled PET phase that imposes deformation constraints to the clean PVDF phase. Under constraints the fracture strength of a ductile phase can increase, as previously found in ductile metals within the brittle ceramic or intermetallic matrices [22].

The analysis above suggests that the fracture strength of carbon-filled polymer blends can be further improved if the clean polymer phase in the carbon-filled polymer blend has a fracture strength higher than PVDF. Therefore, it can be concluded that the intrinsic mechanical properties of the clean

Table 1
Tensile properties of neat polymers and CNT-filled polymers

Materials	PET	PVDF	CNT-filled PET/PVDF (6 vol.% CNT)	CNT-filled PET (6 vol.% CNT)	Improvement of CNT-filled PET/PVDF over CNT-filled PET (%)
Elongation at the rate of break (%)	2.2	1400	5.1	1.2	325
Tensile stress at the rate of yield (MPa)	34	32	–	25	–
Tensile stress at the rate of break (MPa)	34	54	34	25	36

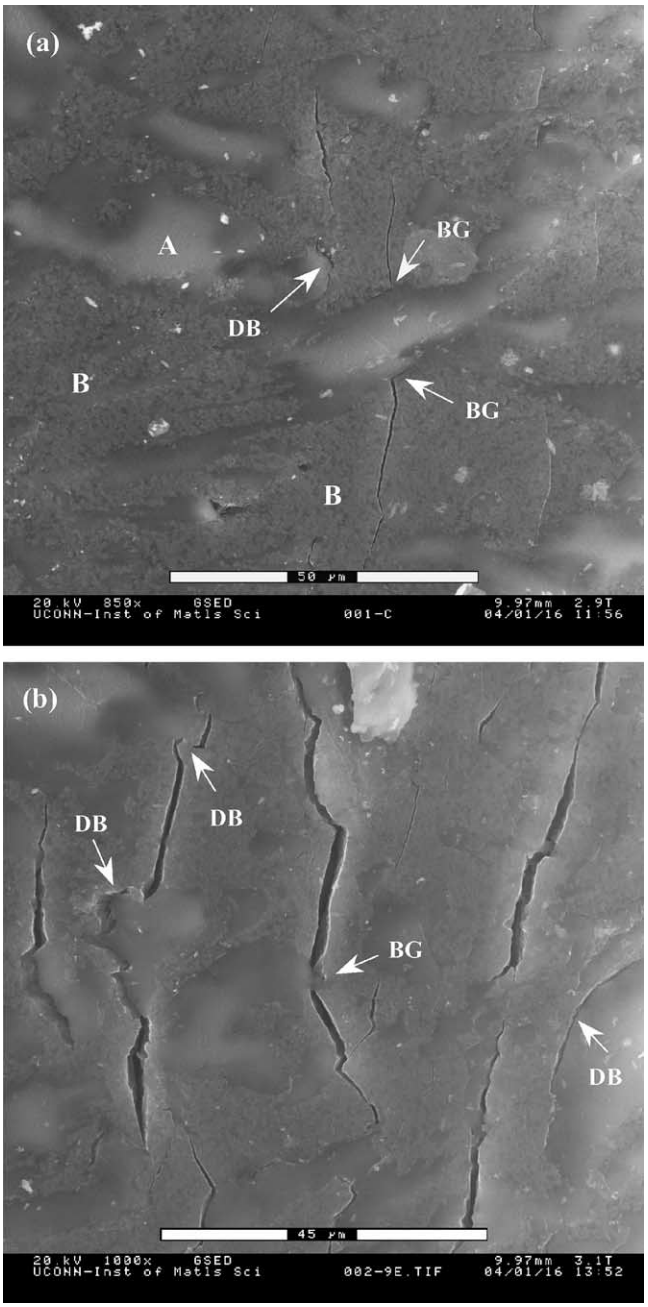

Fig. 6. SEM secondary electron image of crack paths in the CNT-filled PET/PVDF blend with (a) from the region near the shoulder of the tensile specimen and (b) from the central region of the tensile specimen. Region A is the PVDF phase, whereas Region B is the PET with CNT. BG stands for bridging, while DB represents debonding. The loading axis is horizontal.

polymer phase in the carbon-filled binary polymer blend are critical in determining the properties of the resulting composite. Another important conclusion that can be drawn from this study is that the fracture strength of the carbon-filled polymer blend will increase with the increase in the interfacial strength of the two polymer phases. This conclusion is made based on the observation of Fig. 6 which shows that when a crack in the CNT-filled PET phase encounters the clean PVDF phase, the crack either propagates along the PET/PVDF interface or is bridged by the PVDF phase. Therefore, if the interfacial strength of the two polymer phases in the carbon-filled binary polymer blend increases, the fracture strength of the carbon-filled polymer blend will also increase.

The measured electrical conductivities are summarized in Table 2. First of all, it is noted that the CNT-filled PET/PVDF plates exhibit anisotropic conductivity, which is most likely due to the partial alignment of carbon nanotubes in the polymer blend caused by injection flow. During the injection molding process the drag force applied from the die surface to the polymer-carbon nanotube melt mixture can result in partial alignment of carbon nanotubes with their longitudinal axis parallel to the injection flow direction. As a result, the electrical conductivity is higher along the injection flow direction (0.059 S/cm) than that perpendicular to the injection flow direction (0.011 S/cm). The phenomenon of the anisotropic behavior is also present in the injection molded CNT-filled PET (Table 2).

Table 2 also indicates that PET containing 12 vol.% CNT has a conductivity of 0.25 S/cm which is reduced to 0.059 S/cm along the injection flow direction after the CNT-filled PET has injection molded with 50 vol.% PVDF. The reduction in the electrical conductivity is qualitatively consistent with the expectation that the addition of a non-conductor (e.g., PVDF in this case) to a conductive CNT-filled polymer will reduce the conductivity. Since (i) the volume fractions of PVDF and CNT-filled PET are both 50% in the polymer blend studied, (ii) PVDF and PET are immiscible [23], and (iii) most of the carbon nanotubes stay within PET after injection molding, it is reasonable to assume that both PVDF and CNT-filled PET phases have formed self-continuous 3D structures in the CNT-filled PET/PVDF polymer blend. With such 3D structures, the conductive CNT-filled PET network and the non-conductive PVDF phase can be treated as parallel conductors, and the resulting resistivity, ρ, of the CNT-filled PET/PVDF blend can be estimated based on the statistical percolation model proposed by Bueche [24]

$$\rho = \frac{\rho_c \rho_n}{V_n \rho_c + \omega(1 - V_n)\rho_n} \tag{4}$$

where ρ_c and ρ_n are the resistivities of the conductive and non-conductive phases, respectively, V_n the volume fraction of the non-conductive phase, and ω the fraction of the conductive phase being incorporated in the conducting network. The largest possible value for ω is 1, which corresponds to the case where all the CNT-filled PET regions are incorporated into the conductive network. Taking this ideal case of $\omega = 1$ for analysis, the resistivity of the CNT-filled PET/PVDF is estimated to be 8.0 Ω cm if ρ_n for PVDF is taken to be 10^{13} Ω cm [25] and ρ_c for the CNT-filled PET taken from the measured value (4.00 Ω cm).

By comparing the predicted value of resistivity described above with those measured (Table 2), it becomes

Table 2
Electrical conductivities of CNT-filled polymers and polymer blends

	CNT-filled PET[a] (12 vol.% CNT)	CNT-filled PET/PVDF (6 vol.% CNT) (Direction I)	CNT-filled PET/PVDF (6 vol.% CNT) (Direction II)	CNT-filled PET (6 vol.% CNT) (Direction I)	CNT-filled PET (6 vol.% CNT) (Direction II)
Conductivity (S/cm)	0.250	0.059	0.011	0.0023	5.88×10^{-4}
Resistivity, ρ (Ω cm)	4.000	16.95	90.91	430	1700

[a] This CNT-filled PET was prepared via extrusion by Hyperion Catalysis International, Inc., whereas all others were prepared via injection molding by the authors. See Section 2 for details.

obvious immediately that the injection-molded CNT-filled PET/PVDF blend has higher resistivities in both directions than the predicted value for the ideal case. The discrepancy may be attributed to two origins. First, a small amount of the carbon nanotubes may have transferred to the PVDF phase near the PET/PVDF interface during injection molding. As a result of such transfer, the intrinsic resistivity of the CNT-filled PET, ρ_c, could become higher than 4.00 Ω cm used in the calculation, thereby resulting in a higher resistivity of the resulting CNT-filled polymer blend than the predicted value. The second mechanism for the discrepancy is related to the possibility that not all the CNT-filled PET regions have been incorporated into the conductive network. As a result, ω is smaller than 1, which will also lead to a higher resistivity of the resulting CNT-filled polymer blend than the predicted value. Of course, this is consistent with the expectation that not all the CNT-filled PET regions can be incorporated into the conductive network because making connection among all the CNT-filled PET regions during injection molding is a random process.

In summary, the higher resistivity of the resulting CNT-filled PET/PVDF blend than the predicted value of the ideal case may be due to (i) the transfer of a small amount of carbon nanotubes out of the PET phase and (ii) the incomplete connection among all the CNT-filled PET regions. The second mechanism appears to be the dominant one because the 50 vol.% PVDF added to the CNT-filled PET remain about 50 vol.% after injection molding, suggesting little or no transfer of CNT out of the PET phase into the PVDF phase (see Fig. 3).

Finally, it is worthwhile to compare the electrical conductivity obtained in this study with the literature data. Since few CNT-filled PVDF and CNT-filled PET have been published in the open literature, the electrical conductivities of carbon black (CB) filled PVDF polymers in the literature have been used to compare with the present study (Fig. 7). It can be seen that PET with 12 vol.% CNT (i.e. 15 wt.%) has a lower electrical resistivity than the carbon black-filled PVDF with the same carbon loading. The resistivity of PET with 6 vol.% CNT (i.e. 7.5 wt.%), however, is similar to that of the carbon black-filled PVDF. In contrast, the PET/PVDF blend with 6 vol.% CNT exhibits about two orders of magnitude reduction in the resistivity over the carbon black-filled PVDF with the same carbon loading, showing the efficacy of the segregation of carbon in one of the phases in a binary polymer blend. Such an improvement, however, should be treated with caution because carbon nanotubes are typically more efficient in increasing electrical conductivities than carbon black [27,28]. At this stage the relative importance of the carbon morphology and the segregation of carbon in one of the phases in the polymer blend has not been established yet and is currently under investigation.

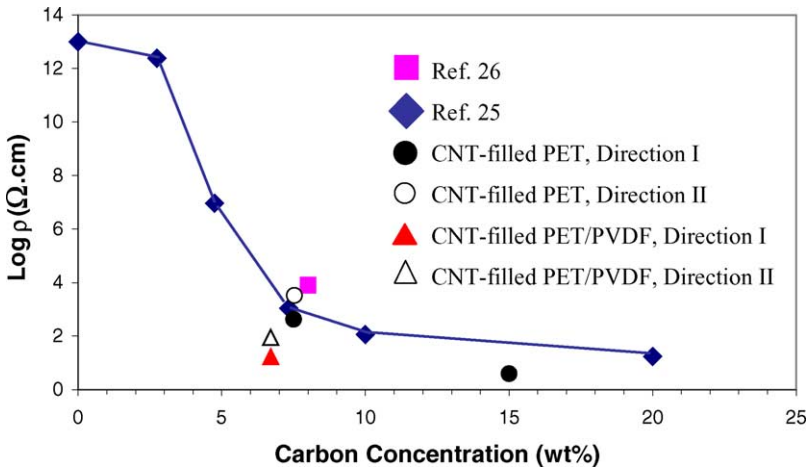

Fig. 7. The resistivities of the CNT-filled PET and CNT-filled PET/PVDF as a function of the carbon concentration. The resistivities of several carbon-filled PVDF composites from the literature are also included for comparison. The line is added as a visual guide only (Sources: [25,26].)

4. Concluding remarks

The CNT-filled PET/PVDF blend exhibits 2500% improvement in electrical conductivity, 36% increase in tensile strength, and 320% improvement in elongation over the CNT-filled PET with the same carbon loading. Such improvements have been related to the formation of a triple-continuous structure achieved through the forced segregation of CNT in the PET phase of the CTN-filled PET/PVDF blend. This CNT-filled PET phase offers an electrical short circuit for the composite, while the clean PVDF phase provides the strength and elongation for the composite. As a result of such a combination, the CNT-filled PET/PVDF has better electrical conductivity, strength and elongation than the CNT-filled PET. The segregation of CNT in the PET phase of the CNT-filled PET/PVDF blend is due to the thermodynamic driving force that favors the segregation of CNT in the PET. Further improvements in electrical and mechanical properties over the CNT-filled PET/PVDF blend are possible. In particular, if a polymer phase, which is free from CNT in the CNT-filled PET-based polymer blend, has a higher fracture strength than PVDF or the interfacial bond strength between PET and PVDF can be increased, the fracture strength of the CNT-filled composite will be further improved. If the polymer phase that hosts CNT has a very low percolation threshold, the electrical conductivity of the CNT-filled polymer blend will be improved further.

Acknowledgements

The authors are indebted to Professors Frano Barbir, Montgomery Shaw and Lei Zhu for insightful discussion over a wide range of the topics related to this research. The assistance provided by Dr. Daniel Goberman in argon ion etching, Dr. Tao Zhou and Mr. Hong Luo in tensile tests, and Mr. Juan Villegas in some of SEM observations is greatly appreciated. Finally, the authors are grateful to the financial support from the U.S. Army (Contract #: DAAB07-03-3-K415) through the Connecticut Global Fuel Cell Center.

References

[1] I. Bar-On, R. Kirchain, R. Roth, Technical cost analysis for PEM fuel cells, J. Power Sources 109 (2002) 71–75.
[2] T.M. Besmann, J.W. Klett, J.J. Henry, E. Lara-Curzio, Carbon/carbon composite bipolar plate for proton exchange membrane fuel cells, J. Electrochem. Soc. 147 (11) (2000) 4083–4086.
[3] P.L. Hentall, J.B. Lakeman, G.O. Mepsted, P.L. Adcock, J.M. Moore, New materials for polymer electrolyte membrane fuel cell current collectors, J. Power Sources 80 (1999) 235–241.
[4] D.P. Davies, P.L. Adcock, M. Turpin, S.J. Rowen, Bipolar plate materials for solid polymer fuel cells, J. Appl. Electrochem. 30 (2000) 101–105.
[5] R. Hornung, G. Kappelt, Bipolar plate materials development using Fe-based alloys for solid polymer fuel cells, J. Power Sources 72 (1998) 20–21.
[6] R.C. Makkus, A.H.H. Janssen, F.A. de Bruijn, R.K.A.M. Mallant, Use of stainless steel for cost competitive bipolar plates in the SPFC, J. Power Sources 86 (2000) 274–282.
[7] T.M. Besmann, J.W. Klett, T.D. Burchell, Carbon composite for a PEM fuel cell, Mater. Res. Soc. Symp. Proc. 496 (1997) 243.
[8] C. Del Rio, M.C. Ojeda, J.L. Acosta, M.J. Escudero, E. Hontanon, L. Daza, New polymer bipolar plates for polymer electrolyte membrane fuel cells: synthesis and characterization, J. Appl. Polym. Sci. 83 (2002) 2817–2822.
[9] G. Marsh, Fuel cell materials, Mater. Today 4 (2) (2001) 20–24.
[10] F. Barbir, J. Braun, J. Neutzler, Properties of molded graphite bipolar plates for PEM fuel cell stacks, J. New Mater. Electrochem. Systems 2 (1999) 197–200.
[11] J. Braun, J.E. Zabriskie Jr., J.K. Neutzler, M. Fuchs, R.C. Gustafson, Fuel Cell Collector Plate and Method of Fabrication, US Patent # 6,180,275.
[12] J.C. Grunlan, W.W. Gerberich, L.F. Francis, Electrical and mechanical behavior of carbon black-filled poly(vinyl acetate) latex-based composites, Polym. Eng. Sci. 41 (11) (2001) 1947–1962.
[13] J.-C. Huang, Review carbon black filled conducting polymers and polymer blends, Adv. Polym. Technol. 21 (4) (2002) 299–313.
[14] C. Xu, Y. Agari, M. Matsuo, Mechanical and electric properties of ultra-high-molecular weight polyethylene and carbon black particle blends, Polym. J. 30 (5) (1998) 372–380.
[15] L. Shaw, Polydisperse carbon-filled polymer blends for fuel cell bipolar plate applications, University of Connecticut Invention Disclosure # 04–010, 4 March 2004.
[16] M. Wu, L. Shaw, A novel concept of carbon-filled polymer blends for applications of PEM fuel cell bipolar plates, Int. J. Hydrogen Energy, March 2004.
[17] F. Gubbels, R. Jerome, P. Teyssie, E. Vanlathem, R. Deltour, A. Calderone, V. Parente, J. Bredas, Selective localization of carbon black in immiscible polymer blends: a useful tool to design electrical conductive composites, J. Macromolecules 27 (1994) 1972–1974.
[18] M. Kozolowski, Electrically conductive structured polymer blends, Polym. Network Blends 5 (4) (1995) 163–172.
[19] M. Sumita, K. Sakata, S. Asai, K. Miyasaka, H. Nakagawa, Dispersion of fillers and the electrical conductivity of polymer blends filled with carbon black, Polym. Bull. 25 (1991) 265–271.
[20] S. Wu, Polymer Interface and Adhesion, Marcel Dekker, Inc., New York, NY, 1982.
[21] B.D. Agarwal, L.J. Broutman, Analysis and Performance of Fiber Composites, second ed., Wiley, New York, 1990.
[22] L. Shaw, R. Abbaschian, On the flow behavior of constrained ductile phases, Metall. Trans. 24A (1993) 403–415.
[23] W.W. Graessley, Phase Behavior of Hydrocarbon Polymer Blends, Institute of Materials Science Distinguished Lecture at University of Connecticut, 28 October 2003.
[24] F. Bueche, Electrical resistivity of conducting particles in an insulating matrix, J. Appl. Phys. 43 (11) (1972) 4837–4838.
[25] G. Wu, C. Zhang, T. Miura, S. Asai, M. Sumita, Electrical characteristics of fluorinated carbon black-filled poly(vinylidene fluoride) composites, J. Appl. Polym. Sci. 80 (7) (2001) 1063–1070.
[26] Z. Zhao, W. Yu, X. He, X. Chen, The conduction mechanism of carbon black-filled poly(vinylidene fluoride) composite, Mater. Lett. 57 (2003) 3082–3088.
[27] O. Meincke, D. Kaempfer, H. Weickmann, C. Friedrich, M. Vathauer, H. Warth, Mechanical properties and electrical conductivity of carbon-nanotube filled polyamide-6 and its blends with acrylonitrile/butadiene/styrene, Polymer 45 (2004) 739–748.
[28] J.K.W. Sandler, J.E. Kirk, I.A. Kinloch, M.S.P. Shaffer, A.H. Windle, Ultra-low electrical percolation threshold in carbon-nanotube-epoxy composites, Polymer 44 (2003) 5893–5899.